The colour-magnitude relation of simulated early-type galaxies as a function of their kinematics

L.J. Zenocratti[1,2], A.V. Smith Castelli[1,2], M.E. De Rossi[3,4] & F.R. Faifer[1,2]

[1] *Facultad de Ciencias Astronómicas y Geofísicas, UNLP, Argentina*
[2] *Instituto de Astrofísica de La Plata, CONICET–UNLP, Argentina*
[3] *Instituto de Astronomía y Física del Espacio, CONICET–UBA, Argentina*
[4] *Facultad de Ciencias Exactas y Naturales, UBA, Argentina*

Contact / ljzenocratti@gmail.com

Resumen / Las galaxias de tipo temprano (ET, por sus siglas en inglés), tanto elípticas como lenticulares, definen la bien conocida secuencia roja o relación color-magnitud (CMR, por sus siglas en inglés) en el diagrama color-magnitud (CMD, por sus siglas en inglés). En este trabajo, presentamos resultados de un estudio de dicha relación a diferentes corrimientos al rojo z en simulaciones numéricas cosmológicas. En particular, exploramos su evolución desde $z = 2$ hasta $z = 0$, seleccionando una muestra de objetos simulados que muestran propiedades similares a las de galaxias ET observadas del universo local. La velocidad de rotación promedio de dichos objetos es utilizada para determinar si su cinemática estelar correlaciona con su posición en el diagrama, así como con otras propiedades. También se analiza la evolución de rotadores rápidos y lentos sobre el CMD a diferentes corrimientos al rojo y los cambios en su comportamiento cinemático. Los resultados aquí mostrados forman parte de un proyecto que apunta a identificar los procesos que originaron la CMR a $z = 0$, realizando una comparación exhaustiva entre galaxias ET simuladas y observadas.

Abstract / Early-type (ET) galaxies (both elliptical and lenticular) define the well-known red sequence or colour-magnitude relation (CMR) in the colour-magnitude diagram (CMD). In this work, we present results of the study of that relation at different redshifts z in cosmological numerical simulations. In particular, we explore its evolution from $z = 2$ to $z = 0$, selecting a sample of simulated objects that display similar properties of observed ET galaxies in the Local Universe. The average rotation speed of those objects is used to determine if their stellar kinematics correlates with their position in the diagram, as well as with other properties. Evolution of fast- and slow-rotators over the CMD at different redshifts and changes in their kinematical behaviour is also analysed. Results shown here are part of a project aimed at identifying the processes that originated the CMR at $z = 0$, performing a comprehensive comparison between simulated and observed ET galaxies.

Keywords / galaxies: elliptical and lenticular, cD — galaxies: kinematics and dynamics — cosmology: theory

1. Introduction

Early-type (ET) galaxies constitute the most numerous type of galaxies in nearby groups and clusters, and their study provide important clues to understand galaxy formation processes. These objects have been widely analysed over time, but there is not yet a global agreement about their origin and the setting up of their properties. Different formation scenarios have been widely discussed for elliptical galaxies, such as gas-rich mergers for giant ellipticals and environmental effects on gas-rich progenitors for gas-poor dwarf ellipticals (e.g. Roediger et al., 2011), dwarf mergers and gas accretion for the assembly of isolated dwarf galaxies (e.g. Janz et al., 2017), and two-phase scenarios for massive elliptical with a fast and early "in situ" star formation phase followed by an extended "ex situ", accretion-driven phase (e.g. Oser et al., 2010). The origin of lenticular galaxies has also been extensively studied in the literature, being environmental processes in the centre of clusters (ram-pressure stripping and harassment, e.g. Moore et al., 1996; Dressler et al., 1997), passive evolution and active galactic nuclei (AGN) effects in field disc galaxies (e.g. van den Bergh, 2009) the more analysed suggestions. Despite the controversies about the formation scenarios of ET galaxies, the observed properties of these systems obey several scaling relations that may involve the physical processes that drive their evolution. For example, in the colour-magnitude diagram (CMD), they trace a well-defined photometric sequence from giant (brighter and redder) to dwarf (fainter and bluer) galaxies. This colour-magnitude relation (CMR) or red sequence has been studied with detail (e.g. Bower et al., 1992; Chen et al., 2010, Smith Castelli et al., 2013; Schombert, 2018), and there is evidence of its universality in groups and clusters of galaxies (e.g. Smith Castelli et al., 2012 and references therein). Although the CMR has been interpreted as a mass-metallicity relation, other factors (such as gas fractions or stellar kinematics) could affect it (e.g. Gallazzi et al., 2006; Graves et al., 2009).

In this work, we present preliminary results of a study on the CMD of simulated ET galaxies as a function of their stellar kinematics. These results represent a first step on the analysis of fast and slow rotation on ET galaxies and their progenitors, trying to provide

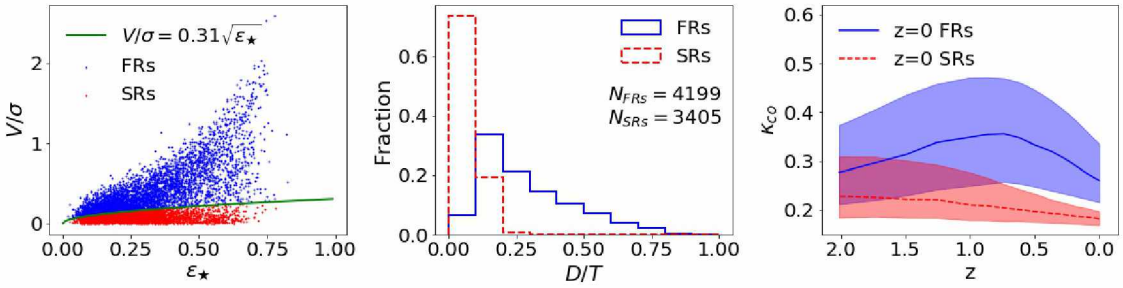

Figure 1: *Left panel*: V/σ vs. $\epsilon_\star$ diagram for EAGLE Ref-L0100N1504 ET galaxies, separating fast-rotators (FRs, blue dots) and slow-rotators (SR, red dots) with the solid curve defined by Emsellem et al. (2011). *Middle panel*: distribution of D/T for the previous sub-samples. *Right panel*: median evolution of morpho-kinematic parameter κ_{co} for the previous sub-sample, with the solid-blue line corresponding to $z = 0$ FRs, and the dashed-red one to the $z = 0$ SRs. The shaded regions enclose the corresponding 25th and 75th percentiles.

clues for the origin and nature of the observed CMR.

2. The EAGLE simulations

We selected galaxies from the catalogues of the EAGLE (Evolution and Assembly of GaLaxies and their Environments) cosmological hydrodynamical simulations (Schaye et al., 2015), which implement a modified version of the GADGET-3 code (Springel, 2005) for formation and evolution of structure, with models calibrated to reproduce the $z \approx 0$ galaxy stellar mass function, the galaxy mass-size relation, and the black hole mass-stellar mass relation (Crain et al., 2015). A standard ΛCDM cosmology was adopted for these simulations, adopting cosmological parameters from Planck Collaboration (2015): $\Omega_L = 0.693$, $\Omega_m = 0.307$, $\Omega_b = 0.048$, and $h = 0.6777$. The EAGLE suite counts with several simulations of different resolutions and physics implementation (see Schaye et al., 2015 and Crain et al., 2015 for details). In this work, we use the intermediate-resolution, reference model (labelled as 'Ref-L0100N1504' in the suite), which simulates a cubic box of co-moving size $L = 100$ cMpc, with an initial baryonic particle mass of 1.2×10^6 M$_\odot$ (1504^3 particles) and a proper softening length of 0.70 pkpc.

3. Sample of simulated ET galaxies

To avoid resolution issues, from the EAGLE Ref-L0100N1504 catalogues we select galaxies with stellar masses $M_\star \geqslant 10^9$ M$_\odot$. The identification of simulated ET galaxies at redshift $z = 0$ follows the criteria of Zenocratti et al. (2020), which impose constraints to the observed specific star formation rate ($sSFR$) and star-forming gas fraction $f_g = M_{\rm SF\ gas}/(M_{\rm SF\ gas} + M_\star)$. We select then $z = 0$ galaxies with $sSFR < 10^{-11}$ yr^{-1} and $f_g < 0.1$. Systems that fulfil these conditions define our sample of simulated ET galaxies, composed of 7604 objects. As shown in Zenocratti et al. (2020), the colour-magnitude diagram of this simulated sample agrees with the one corresponding to observed ET galaxies in the Virgo cluster. The parameters we use to characterize stellar morphology and kinematics are fully described in Thob et al. (2019): we use the stellar rotation-to-velocity dispersion ratio (V/σ), ellipticity of the stellar body ($\epsilon_\star$), the disc-to-total stellar mass ratio (D/T), and the fraction of kinetic energy invested in ordered co-rotation (κ_{co}). We refer the reader to Thob et al. (2019) for complete details about these parameters.

4. Results

We divide our sample of simulated ET galaxies in fast- and slow-rotators as shown in the left panel of Fig. 1, following Emsellem et al. (2011): if $V/\sigma \geqslant 0.31\sqrt{\epsilon_\star}$ ($V/\sigma < 0.31\sqrt{\epsilon_\star}$), the galaxy is classified as a FR (SR). Our sample consists of 4199 FRs and 3405 SRs. The middle panel of Fig. 1 shows the distribution of D/T parameter for each sub-sample. Most of our SRs exhibit values of $\epsilon_\star \lesssim 0.4$ and $D/T \lesssim 0.1$, which suggests that these might be spheroid-like, bulge-dominated systems, i.e. elliptical galaxies. In the FRs sub-sample, almost half of the galaxies have $D/T \lesssim 0.3$, hence some elliptical galaxies might be present here too; the "tail" in the distribution of these galaxies towards the highest $\epsilon_\star$ and the highest V/σ corresponds to the highest values of D/T, suggesting that these disc-dominated ET could be associated to lenticular galaxies. This trends agree with results of Krajnović et al. (2013) for observed ET galaxies. The average evolution of the rotation-to-total energy ratio κ_{co} for $z = 0$ SRs and FRs is shown in the left panel of Fig. 1. At a given redshift z, the progenitors of each galaxy in the corresponding sub-sample are identified, and then the median value of κ_{co} at that redshift is calculated. The curves represent then the median evolution of κ_{co}, with the shaded regions enclosing the 25th and 75th percentiles. In the $z = 0$ SRs sub-sample, κ_{co} keeps below the value $\kappa_{co} \approx 0.22$ on average, with a decreasing trending towards smaller z, suggesting that $z = 0$ SRs are typically galaxies that show small rotation at every z. On the other hand, for the FRs sub-sample, κ_{co} tends to increase on average up to $z \sim 1$, and from that moment on, it decreases up to $z = 0$. This suggests that rotation tends to become more relevant with time in FRs, but they go through some process at recent times that mitigates the increment. A detailed analysis of physical processes leading to that behaviour will be presented in a future work.

The upper (lower) panels of Fig. 2 show the evolution of our simulated sub-samples of ET galaxies that

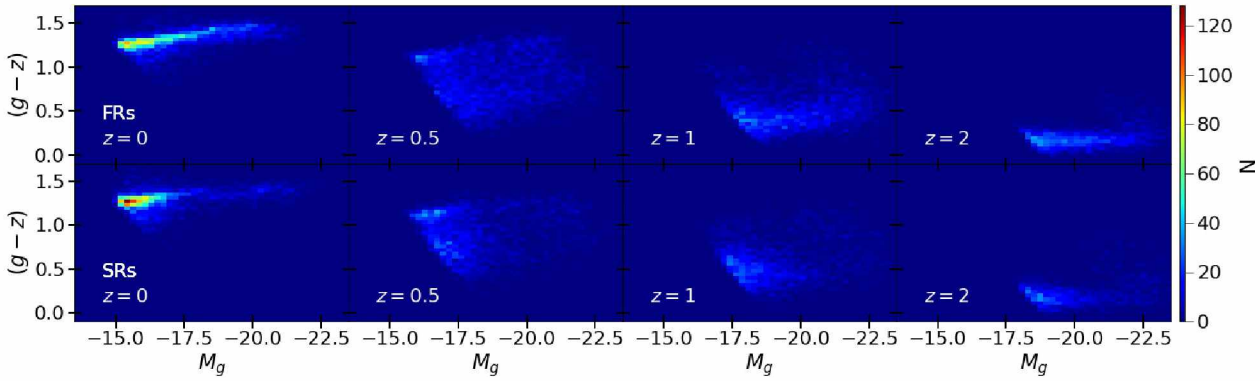

Figure 2: CMD of $z = 0$ fast-rotators (*top panels*) and slow-rotators (*bottom panels*) and their respective progenitors at different redshifts, colour-coded according to the number N of galaxies.

are fast- (slow-) rotators at $z = 0$ on the $(g - z)$ vs. M_g diagram. At $z = 2$, both sub-samples are located approximately in the region with $-22 \lesssim M_g \lesssim -18$ and $(g-z) \approx 0.1$, with the progenitors of SRs predominantly in the faint-end of M_g. Towards $z = 1$, the sub-samples move alike to fainter and redder regions of the CMD, but the progenitors of FRs are more dispersed along the magnitude range, towards brighter regions of the CMD. At $z = 0.5$, there is an evident scatter in both colour and luminosity for the FRs progenitors. These scatters might be associated with the physical processes that prevent the increase of rotation in this galaxies. The same scatter in colour is present for the SRs progenitors, but their magnitudes are bounded to a quite smaller region. Finally, at $z = 0$, both FRs and SRs are found more densely on the faint-end of the red sequence ($-17 \lesssim M_g \lesssim -15$), while the brightest and reddest tail of the red sequence at $z = 0$ ($M_g \leqslant -19$, $(g - z) \geqslant 1.3$) is populated mostly by FRs (there are 682 FRs and 315 SRs in that region of the z=0 CMD). At this time, the scatter in colour has reduced for both samples, and we can say that the CMR is well-established.

5. Summary and further work

We selected a sample of simulated ET galaxies extracted from the EAGLE cosmological hydrodynamical simulations, with criteria based on their observed properties, that leads to a consistency between simulated and observed CMDs. Using the V/σ parameter, we divided our sample in fast- and slow-rotators (FRs and SRs, respectively), following Emsellem et al. (2011). According to the D/T and $\epsilon_\star$ parameters, SRs are mostly elliptical galaxies, while FRs include both elliptical and lenticular galaxies. The average evolution of kinematical parameters suggests that SRs have always low rotation, while in FRs it tends to increase, but some process at low redshift ($z \sim 1$) inverts the trend. Comparing the CMDs at $z = 0$, both kind of rotators are more densely located in the faint-end of the CMR, but in the brightest and reddest region of the CMR, the FRs dominates the population of galaxies. The evolution on the CMD of progenitors of FRs and SRs is somewhat similar, although at recent times ($1 \gtrsim z \gtrsim 0.5$) the luminosity of the former covers a wider range.

In a future work, the criteria used to select ET galaxies from simulations will be refined, by means of comprehensive comparisons with observations. Also, more sophisticated criteria to carry out the FRs/SRs separation using other kinematical diagnosis will be tested and implemented.

Acknowledgements: We acknowledge Asociación Argentina de Astronomía for giving us the space to show our results. We acknowledge support from PICT-2015-3125 of ANPCyT, PIP 112-201501-00447 of CONICET and G151 of UNLP (Argentina). We acknowledge the Virgo Consortium for making their simulation data available. The EAGLE simulations were performed using the DiRAC-2 facility at Durham, managed by the ICC, and the PRACE facility Curie based in France at TGCC, CEA, Bruyères-le-Châtel. This work used the DiRAC@Durham facility managed by the Institute for Computational Cosmology on behalf of the STFC DiRAC HPC Facility (www.dirac.ac.uk). The equipment was funded by BEIS capital funding via STFC capital grants ST/P002293/1, ST/R002371/1 and ST/S002502/1, Durham University and STFC operations grant ST/R000832/1. DiRAC is part of the National e-Infrastructure.

References

Bower R.G., Lucey J.R., Ellis R.S., 1992, MNRAS, 254, 601
Chen C.W., et al., 2010, ApJS, 191, 1
Crain R.A., et al., 2015, MNRAS, 450, 1937
Dressler A., et al., 1997, ApJ, 490, 577
Emsellem E., et al., 2011, MNRAS, 414, 888
Gallazzi A., et al., 2006, MNRAS, 370, 1106
Graves G.J., et al., 2009, ApJ, 698, 1590
Janz J., et al., 2017, MNRAS, 468, 2850
Krajnović D., et al., 2013, MNRAS, 432, 1768
Moore B., et al., 1996, Nature, 379, 613
Oser L., et al., 2010, ApJ, 725, 2312
Planck Collaboration, 2015, A&A, 594, A13
Roediger J.C., et al., 2011, MNRAS, 416, 1996
Schaye J., et al., 2015, MNRAS, 446, 521
Schombert J.M., 2018, AJ, 155, 69
Smith Castelli A.V., et al., 2012, MNRAS, 419, 2472
Smith Castelli A.V., et al., 2013, ApJ, 772, 68
Springel V., 2005, MNRAS, 364, 1105
Thob A.C.R., et al., 2019, MNRAS, 485, 972
van den Bergh S., 2009, ApJ, 702, 1502
Zenocratti L.J., et al., 2020, BAAA, 61B, 168